

do not conserve quasiparticle number are allowed (Fermi resonance). This phenomenon was first observed for phonons in quartz and aluminum phosphate,¹⁰ and treated by Ruvalds and Zawadowski¹⁰ via many-body techniques. A more detailed discussion of the two-magnon line shape in RbCoF_3 will be given in a subsequent paper, where a comparison with TlCoF_3 will be made.

ACKNOWLEDGMENTS

The authors thank P. Moch and C. Dugautier for a copy of their manuscript prior to publication. Professor Moch is also thanked for comments on the manuscript, and the authors appreciate the sample preparation and orientation by Mme. Lenain.

*Permanent address: Service de Physique, Université du Mans, Le Mans, France.

¹Work supported in part by NSF Contract No. GH-34681.

¹References to inelastic scattering studies on these two crystal classes are found in T. M. Holden *et al.*, *J. Phys. C* **4**, 2127 (1971).

²R. M. MacFarlane, *Phys. Rev. Lett.* **25**, 1454 (1970); R. M. MacFarlane and H. Morawitz, *Phys. Rev. Lett.* **27**, 151 (1971).

³J. H. Christie and D. J. Lockwood, in *Light Scattering in Solids*, edited by M. Balkanski (Flammarion, Paris, 1971), p. 145.

⁴Y. Allain *et al.*, *J. Phys. (Paris)* **32**, C1-611 (1971);

J. Nouet *et al.*, *J. Cryst. Growth* **8**, 94 (1971).

⁵W. J. L. Buyers *et al.*, *J. Phys. C* **4**, 2139 (1971); in *Proceedings of the Eleventh International Conference on Low Temperature Physics*, edited by J. F. Allen, D. M. Finlayson, and D. M. McCall (University of St. Andrews, St. Andrews, Scotland, 1969), p. 1330.

⁶P. Moch and C. Dugautier (unpublished).

⁷J. F. Scott and J. Nouet, *Phys. Lett. A* **39**, 385 (1972).

⁸P. A. Fleury and R. Loudon, *Phys. Rev.* **166**, 514 (1968).

⁹P. A. Fleury, *Phys. Rev. Lett.* **21**, 151 (1968).

¹⁰J. F. Scott, *Phys. Rev. Lett.* **24**, 1107 (1971); *Phys. Rev. Lett.* **21**, 907 (1968); J. Ruvalds and A. Zawadowski, *Phys. Rev. Lett.* **24**, 1111 (1971); *Phys. Rev. B* **2**, 1172 (1970).

¹¹P. A. Fleury and P. D. Lazay, *Phys. Rev. Lett.* **26**, 1331 (1971).

¹²P. A. Fleury and J. M. Worlock, *Phys. Rev.* **174**, 613 (1968).

¹³R. J. Elliott *et al.*, *Phys. Rev. Lett.* **21**, 147 (1968); P. A. Fleury, *Phys. Rev. Lett.* **21**, 151 (1968); *Int. J. Magn.* **1**, 75 (1970), and references therein.

¹⁴S. Racine, J. Cipriani, and C. Pontikis, *C.R. Acad. Sci. B* **274**, B16 (1972).

¹⁵W. J. Byra, P. M. Richards, and R. R. Bartkowski, *Phys. Rev. Lett.* **28**, 826 (1972). In an earlier paper on NiF_2 [P. A. Fleury, *Phys. Rev.* **180**, 591 (1969)], it was reported that the integrated intensity of magnon-pair scattering decreased with increasing T . This error was due to the failure to correct for temperature-dependent absorption and has very recently been corrected [W. J. Byra *et al.* (unpublished)].

¹⁶R. T. Harley, W. Haynes, and S. R. P. Smith, in Ref. 3, p. 357.

¹⁷R. J. Elliott, in Ref. 3, p. 354.

¹⁸J. Kanamori, *J. Appl. Phys. Suppl.* **31**, 1415 (1960); see also, B. Halperin and R. Engleman, *Phys. Rev. B* **3**, 1698 (1971).

¹⁹K. A. Hay and J. B. Torrance, Jr., *Phys. Rev. B* **2**, 746 (1970).

²⁰J. B. Torrance and J. C. Slonczewski, *Phys. Rev. B* **5**, 4648 (1972).

²¹T. Moriya, *J. Appl. Phys.* **39**, 1042 (1968).

²²V. S. L'vov, *Fiz. Tverd. Tela* **10**, 451 (1968) [*Sov. Phys.-Solid State* **10**, 354 (1968)].

Uniaxial Stress Experiments and Magnetoelastic Interactions in Manganese Oxide

D. Bloch and R. Maury

Laboratoire de Magnétisme, Centre National de la Recherche Scientifique, B.P. 166, 38042-Grenoble-Cedex, France

(Received 4 December 1972)

We have measured the thermal expansion and the Néel temperature of a single crystal of manganese oxide as a function of uniaxial stress applied along a (111) axis. It is shown that under well-defined experimental conditions, the antiferromagnetic-paramagnetic transition is of first order. The experimental results are used to study magnetoelastic interactions and magnetoelastic effects in manganese oxide.

INTRODUCTION

Magnetoelastic interactions arise from the modulation with interatomic distances of magnetic and cohesive energies. A large variety of physical properties of magnetic substances are attributed to these interactions. However, analysis of these properties by means of adjustable magnetoelastic coefficients does not prove unambiguously the mag-

netoelastic nature of these properties, so that other processes are equally plausible in some cases. Hydrostatic-pressure or uniaxial-stress experiments are often very suitable in order to clarify the nature and the effects of magnetoelastic interactions in magnetic solids.¹ This paper is specifically concerned with magnetoelastic interactions in antiferromagnets. We have chosen manganese oxide, as an example, since it presents a large vari-

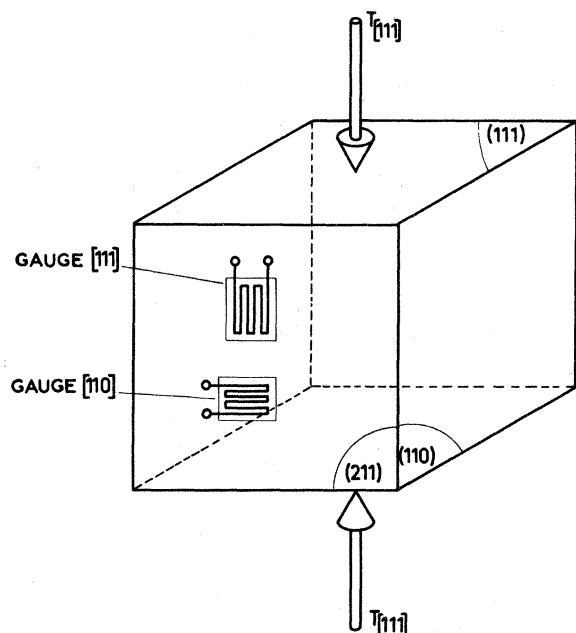


FIG. 1. Crystallographic orientation of the MnO cubic sample used in the experiment.

ety of physical properties which have been attributed to these interactions.²

Section I describes the experimental results obtained by measuring thermal expansion and the Néel temperature as a function of uniaxial stress. The results are analysed in Sec. II using the molecular-field approximation. In Sec. III the results of this analysis are used to discuss various physical properties which are presumed to be of magnetoelastic origin.

I. EXPERIMENTAL RESULTS

Manganese oxide possesses, at room temperature, a cubic NaCl structure. The antiferromagnetic Néel temperature is at $\Theta_N \approx 118$ K. In order to study the effect of stress on the Néel temperature and on thermal expansion, a single crystal cube of manganese oxide was prepared as indicated in Fig. 1.

The [111], [110] and [211] crystallographic axes are perpendicular to the cubic faces, within 0.1° . The MnO sample is a single crystal with a specified manganese purity 99.5% purchased from LETI, Centre d'Etudes Nucléaires, Grenoble. Stress is applied using an apparatus similar to that described in Ref. 1. Temperature is determined using a calibrated AsGa diode. The probable error on the absolute value of the temperature is approximately ± 0.05 K in the 77–300-K temperature range. Two strain-gauges³ are fixed to measure strains along the [111] and [110] directions in the (211) plane. Stress is applied normal to the (111)

plane. This direction has been chosen since x-ray measurements done on MnO powders indicate that MnO contracts along a [111] direction when cooled below its Néel temperature.^{4–6} For the data shown in Figs. 2 and 3, stress was applied in the high-temperature paramagnetic range and was maintained constant during cooling and warming. Between two sets of experiments, stress was released and the sample was annealed for several hours at room temperature. Results obtained according to this procedure are reproducible, with no stress hysteresis effects (Figs. 2 and 3). One observes an increase of the Néel temperature of MnO at a rate of 3.84 ± 0.04 K/kbar (Fig. 4).

During these experiments, a thermal hysteresis was noted in the Néel temperature of MnO from experiments performed at constant stress. This temperature hysteresis of the Néel temperature is of approximately 1.1 K, independent of the applied stress above 40 bar. One observes a length discontinuity at the Néel temperature. The amplitude of this discontinuity increases with increasing stress. Thus, the first-order character of the magnetic transition is clearer at high stress. When the stress is released in the magnetically ordered region, at 77 K, the single crystal does not keep its geometrical dimension, but takes intermediary dimensions, between that obtained with no stress and that obtained before releasing the mechanical stress. When the maximum stress

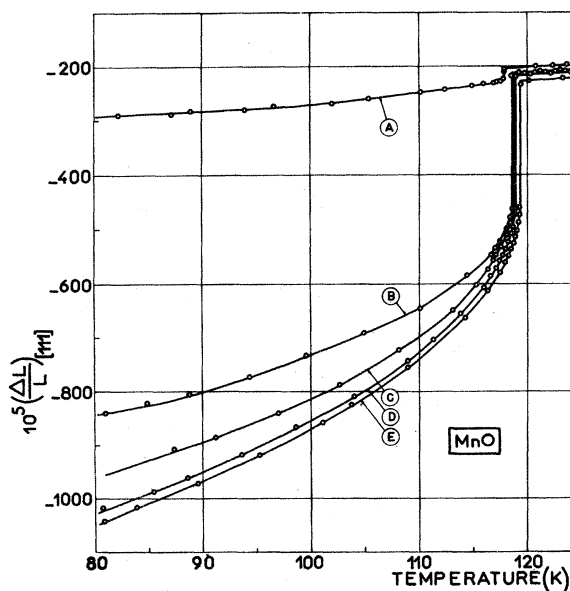


FIG. 2. Thermal variation of the length of MnO as determined in a [111] direction for various stresses T applied along the [111] direction to the (111) faces of the cubic sample, for increasing temperatures. A = 0 bar; B = 53 bar; C = 95 bar; D = 163 bar; E = 269 bar; $\Delta L/L = 0$ at room temperature (293 K) without stress.

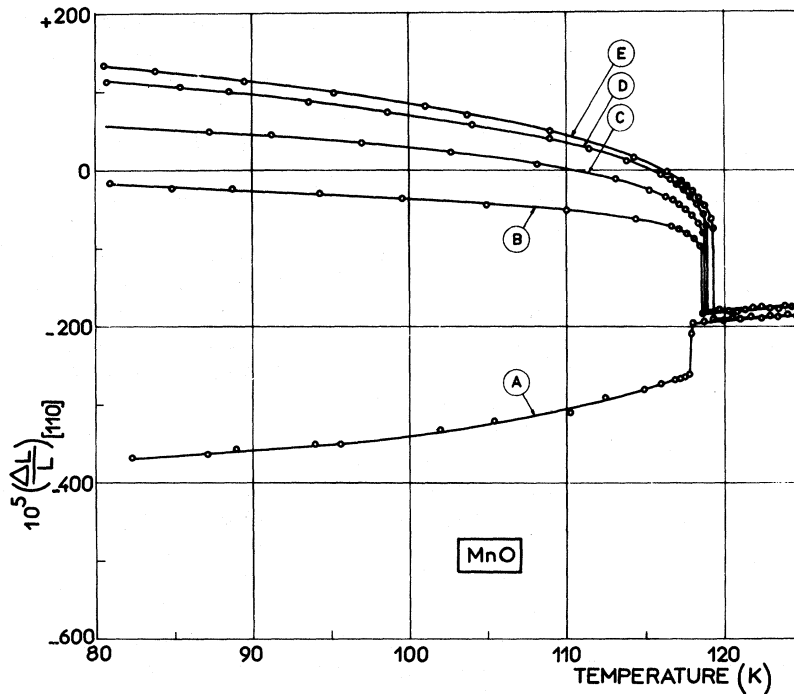


FIG. 3. Thermal variation of the length of MnO as determined in a [110] direction for various stresses applied along the [111] direction to the (111) faces of the cubic sample for increasing temperatures. A=0 bar; B=53 bar; C=95 bar; D=163 bar; E=269 bar; $\Delta L/L=0$ at room temperature (293 K) without stress.

(270 bar) is applied to an unstressed crystal at 77 K, the dimensions obtained are identical to those obtained from cooling at constant 270 bar stress. In a previous set of experiments⁷ the variation with hydrostatic pressure of the Néel temperature of MnO was determined. The variation of the Néel temperature with hydrostatic pressure was observed to be only 0.30 ± 0.02 K/kbar.

II. MAGNETOELASTIC INTERACTIONS

Although the uniaxial strains exceeded 10^{-5} , in the following analysis we assume they are derived from T , the stress applied to the (111) plane along the [111] direction, by the second-order elastic stiffness moduli c_{ij} .

If a is the value of the crystallographic unit-cell cubic edge of MnO, the distance between nearest-Mn neighbors is $a/\sqrt{2}$ and the distance between next-nearest Mn ions is a . Under the application of the [111] stress, the 12 nearest-Mn neighbors of a manganese ion separate into two parts. Six belong to the (111) plane and therefore get farther apart with a distance

$$r_{1,+} = (a/\sqrt{2})(1 + e_{xx} - \frac{1}{2}e_{yy}). \quad (1a)$$

The distance between a manganese ion and its other six neighbors decreases and becomes

$$r_{1,-} = (a/\sqrt{2})(1 + e_{xx} + \frac{1}{2}e_{yy}); \quad (1b)$$

the distance between the six next-nearest neighbors is then

$$r_2 = a(1 + e_{xx}), \quad (2)$$

where the components of the strain tensor are

$$e_{xx} = e_{yy} = e_{zz} = T/3(c_{11} + 2c_{12}), \quad (3a)$$

$$e_{xy} = e_{xz} = e_{yz} = T/3c_{44}. \quad (3b)$$

In the conditions of the experiment, where T is negative and small, the cubic angles become $\frac{1}{2}\pi + \alpha$, with $\alpha = T/3c_{44}$, which corresponds to a slight rhombohedral distortion of the cubic crystallographic cell. Under the application of an hydrostatic pressure p the crystal deforms isotropically, with

$$e_{xx} = e_{yy} = e_{zz} = P/(c_{11} + 2c_{12}). \quad (4)$$

The manganese cations Mn^{2+} have an electronic $S = \frac{5}{2}$ state. Thus, crystal field effects are weak and will be neglected. Hence, the Hamiltonian of the magnetic system is of the Heisenberg type:

$$H = -2 \sum_{(ij)} J_{ij} \vec{S}_i \cdot \vec{S}_j, \quad (5)$$

where the summation is made on pairs of magnetic atoms of spin \vec{S}_i and \vec{S}_j . We call J_l the exchange interaction coefficient between first-nearest neighbors and z_l the number of l th neighbors.

In the magnetically ordered temperature range the magnetic structure can be described as a second-order type antiferromagnet,⁸ where a magnetic ion of spin S has six next-nearest neighbor spins with antiparallel spins ($\uparrow\downarrow$). Of its 12 nearest neighbor spins, six are parallel ($\uparrow\uparrow$) and six antiparallel ($\uparrow\downarrow$). We will only consider exchange interactions between these neighbors. Within the molecular field approximation, the Néel temperature can

be written

$$\Theta_N = -4S(S+1)J_2. \quad (6)$$

In the absence of applied stress, the MnO single crystal separates below Θ_N , into the so-called T domains.^{9,10}

Inside a T domain, the spins belonging to a (111) plane are ferromagnetically aligned, whereas neighboring (111) planes have antiparallel spins. The spontaneous distortion corresponds to an increase of the distance between nearest neighbors in a (111) plane, whereas nearest neighbors belonging to neighboring (111) plane become nearer.

Each T domain corresponds to one of the four possible stackings along the four equivalent $\langle 111 \rangle$ type axes. Applying a stress along a $[111]$ axis then favors that T domain which contracts in the direction of applied stress, as had been observed in NiO.^{9,10} For a single T domain, the Néel temperature is then

$$\Theta_N = -4S(S+1)(J_2 + J_{1,\parallel} - J_{1,\perp}), \quad (7)$$

where $J_{1,\parallel}$, $J_{1,\perp}$, and J_2 are, respectively, the exchange interaction coefficients between antiparallel nearest neighbors at distance $r_{1,\perp}$, parallel nearest neighbors at distance $r_{1,\parallel}$, and antiparallel next-nearest neighbors at distance r_2 . The value of J_1 can be deduced from the value of the magnetic susceptibility at the Néel temperature once J_2 is determined using Eq. (6):

$$\chi(T=\Theta_N) = -N\mu_B^2/3(J_1 + J_2), \quad (8)$$

where N is the number of magnetic atoms.

Hydrostatic pressure p or uniaxial stress T modify the interatomic distances, and thus modify the exchange interaction coefficients J_1 and J_2 .

These modifications will be described by the coefficients

$$j_1 = \frac{dJ_1/J_1}{dr_1/r_1}, \quad j_2 = \frac{dJ_2/J_2}{dr_2/r_2},$$

where j_1 describes the modification of J_1 when a stress is applied along a $[111]$ axis and modifies, at the same time, the interatomic distances and the crystallographic angles. Under the application of hydrostatic pressure or uniaxial stress, the path $\text{Mn}^{2+} - \text{O}^2 - \text{Mn}^{2+}$ between second neighbors remains a 180° path, and the interatomic distances alone are changed. The variations of the Néel temperature should thus satisfy the pressure derivatives of Eqs. (6) and (7):

$$\frac{d\Theta_N}{dp} = -\frac{4S(S+1)j_2J_2}{(c_{11} + 2c_{12})}, \quad (9a)$$

$$\frac{d\Theta_N}{dT} - \frac{1}{3} \frac{d\Theta_N}{dp} = \frac{4S(S+1)j_1J_1}{3c_{44}}. \quad (9b)$$

The above equations neglect the variations of interatomic distances due to the thermal expansion when the temperature is varied by $d\Theta_N$. Thus j_1 and j_2 can be easily deduced from the variations of the Néel temperature Θ_N with hydrostatic pressure or $[111]$ stresses.

From Eqs. (6) and (8) one deduces

$$J_1 = -7.2 \text{ K}, \quad J_2 = -3.4 \text{ K}.$$

From the values $\Theta_N = 118 \text{ K}$ and $\chi(T=\theta_N) = 59 \times 10^{-4} \text{ emu/mole}$.¹¹ Such a calculation is done under the assumption that θ_N is a true Néel temperature and not a first-order transition temperature. In the following the temperature of the first-order transition as extrapolated to zero stress will be

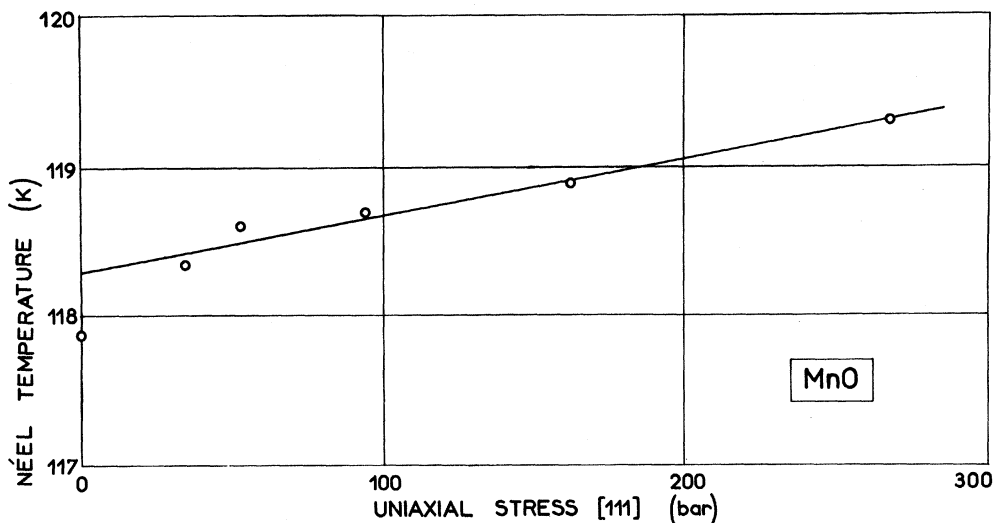


FIG. 4. Variation of the Néel temperature of MnO with stress applied along the $[111]$ direction to the (111) faces of the sample. The Néel temperature is determined from the results given in Figs. 2 and 3.

taken as the Néel temperature of the undistorted state.

In the absence of more specific elastic constant data we assume for the compressibility that the value¹²

$$K = 3/(c_{11} + 2c_{12}) = 0.70 \times 10^{-6} \text{ bar}^{-1}$$

determined at ambient temperatures is independent of temperature. The c_{44} coefficient has been determined in the vicinity of the Néel temperature, in the paramagnetic region.¹³ We obtain at Θ_N the value $c_{44} = 0.57 \times 10^6$ bar; c_{44} is same under adiabatic or isothermal conditions. This value is determined by extrapolation to Θ_N of the experimental ultrasonic data in the paramagnetic region, since the elastic coefficients to use in Eq. (9) are the elastic coefficients which would describe the elastic behavior of the nonmagnetic crystal. One thus obtains

$$j_1 = -25, \quad j_2 = -12.$$

This j_2 value is very similar to that $j \approx -10$ observed for various compounds with superexchange interactions.^{14,15} The coefficient j_1 is, in contrast, associated with angular variations of the crystallographic axis. The large value of j_1 compared to that of j_2 indicates the possibility of direct exchange interactions between first-neighbor magnetic ions. Owing to the large value of j_1 , the magnetic-ordering temperature can thus be of the first-order type.¹⁶

III. SPONTANEOUS MAGNETOSTRICTION

In the antiferromagnetic state the MnO single crystal, when submitted to low stresses, behaves like a very soft material (Figs. 2 and 3) with large dimensional changes associated with small increases of the applied stress. For larger stresses, above 200 bar, the variation of the crystal dimensions with applied stresses corresponds to that which could be expected from the values of the elastic coefficients in the paramagnetic range. One can then consider that MnO, above 200 bar, is mostly composed of a single T domain. In fact, the thermal variation of its length as measured along [111] and [110] directions (Figs. 2 and 3) is then very similar to that calculated from x-ray diffraction experiments performed on a powder sample⁵ (Fig. 5). In contrast, the thermal variation of its length as measured along the same directions in the absence of applied stress is similar to that observed for powder, in the [100] direction, which means that, without stress, the crystal possesses an isotropic thermal expansion in the low-temperature magnetically ordered range. This corresponds to an equipartition between the various T domains which are then present. At least at low temperature, the 20–100 μ powder used for x-ray experiments^{5,11} can be considered as single- T -do-

main particles. The similarity which exists between the single crystal under high stress and the powder does not remain at higher temperatures, below the Néel temperature. In this case, T domains can be simultaneously present in a single particle, since their elastic distortion energy decreases rapidly in the vicinity of the Néel temperature. Owing to the elastic interaction between the T domains, distortion effects are thus much weaker, and the first order character of the magnetic transition can be obscured or can even disappear. This is in agreement with the magnetic after-effect properties discovered in the study of the susceptibility of MnO in the neighborhood of its Néel temperature.¹¹

When submitted to compression $\delta a/a$ and to shear α , the elastic energy per mole of volume V_m is

$$W_{el} = \frac{3}{2} V_m (c_{11} + 2c_{12}) (\delta a/a)^2 + c_{44} \alpha^2. \quad (10)$$

The variation of the magnetic energy is the magnetoelastic energy

$$W_{me} = 6N S_z^2 [j_2 J_2 (\delta a/a) - j_1 J_1 \alpha]. \quad (11)$$

Minimization of the free energy leads to the equilibrium condition^{17,18}

$$\alpha = \frac{2N j_1 J_1 S_z^2}{V_m c_{44}}, \quad (12a)$$

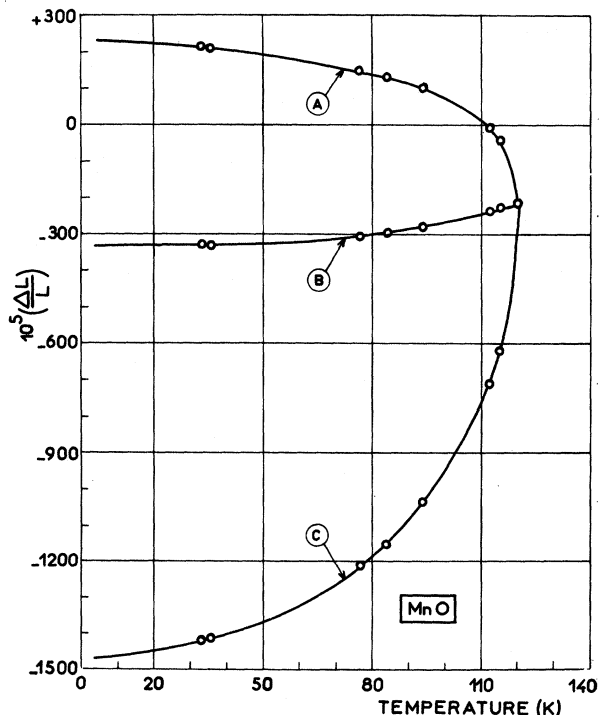


FIG. 5. Thermal variation of the length of MnO in the [111]_C, [110]_A, and [100]_B directions, deduced from Ref. 5. $\Delta l/l = 0$ at room temperature (293 K) without stress.

$$\frac{\delta a}{a} = -\frac{2N}{V_m} \frac{j_2 J_2 S_Z^2}{c_{11} + 2c_{12}}, \quad (13a)$$

where α depends on j_1 and $\delta a/a$ on j_2 . Using Eqs. (9), (12a) and (13a) can also be written

$$\alpha = -\frac{N}{V_m} \frac{3S_Z^2}{2S(S+1)} \left(\frac{d\Theta_N}{dT} - \frac{1}{3} \frac{d\Theta_N}{dp} \right), \quad (12b)$$

$$\frac{\delta a}{a} = \frac{N}{V_m} \frac{S_Z^2}{2S(S+1)} \frac{d\Theta_N}{dp}. \quad (13b)$$

The values of $\delta a/a$ and α calculated from Eqs. (12b) and (13b) for $T=0$ K are -0.7×10^{-3} and 2.4×10^{-2} , respectively, with $N/V_m = 4.60 \times 10^{22}$ per cm^3 and $S_Z = S = \frac{5}{2}$. These are to be compared to the experimental values for $\delta a/a$ of -1.25×10^{-3} (Ref. 5) and -1.1×10^{-3} (Ref. 6) and for α of 1.12×10^{-2} (Ref. 5) and 1.1×10^{-2} (Ref. 6). The agreement is only qualitative, which is presumably owing to the molecular field approximation.⁶ In fact, analysis of the experimental $\delta a/a$ and α data using Green's function theory leads to the values $j_1 = -23$ and $j_2 = -11$, which are close to the values $j_1 = -25$ and $j_2 = -12$ determined in Sec. II. Also, elastic constant values used in the latter calculation are slightly different than those used in deriving j_1 and j_2 from Eqs. 9.

Inelastic-neutron experiments on MnO single-crystal and three-parameter fits of the pertinent data (J_{11} , J_{12} , and J_2) lead to the value¹⁹

$$(J_{11}, -J_{12})/J_1 = 0.29 \text{ at } 4.2 \text{ K.}$$

In a linear approximation this ratio should equal $j_1 \alpha = -0.28$, with $j_1 = -25$ and $\alpha = 1.12 \times 10^{-2}$.

There is thus a disagreement between the sign of $J_{11}, -J_{12}$, as determined from analysis of inelastic-neutron experiments and from direct magnetoelastic evaluation. It would certainly be useful to perform the same inelastic-neutron experiments on a single crystal under stress, in order to get an uni-

form crystallographic distortion.

Magnetoelastic interactions give rise to a temperature dependent perpendicular magnetic susceptibility. At high magnetic fields the direction of antiferromagnetism is perpendicular to the direction of the applied magnetic field,²⁰ and the magnetic susceptibility is

$$\chi(T) = -\frac{N\mu_B^2}{3[J_{11}(T) + J_2(T)]}. \quad (8')$$

Most of the thermal variation of χ results from that of J_1 , and one has, for instance,

$$\frac{\chi(0)}{\chi(T_N)} = \frac{J_1 + J_2}{J_1(0) + J_2} \approx 1 + \frac{\alpha}{2} \frac{j_1 J_1}{J_1 + J_2}.$$

With the numerical values $\alpha = 1.12 \times 10^{-2}$, $j_1 = -25$, $J_1 = -7.2$ K, and $J_2 = -3.4$ K one obtains

$$\chi(0)/\chi(T_N) = 0.90,$$

which compares favorably with the experimental value (11)

$$\chi(T=0\text{K})/\chi(T=T_N) = 0.89.$$

CONCLUSION

We have demonstrated unambiguously the first-order nature of the magnetic-ordering transition of a single T domain of manganese oxide. We have shown why the first-order character of this transition was obscured in the case of powdered samples or stress-free single crystals. Furthermore, we have shown that uniaxial stress experiments are of value in quantitative analysis of the magnetoelastic interactions in manganese oxide and related effects such as the spontaneous magnetostriction which occurs in the magnetically ordered state.

ACKNOWLEDGMENT

We wish to thank R. Pauthenet and E. Fisher for informative discussions and comments.

¹H. Bartholin and D. Bloch, Phys. Rev. **188**, 845 (1969).

²H. Bartholin, D. Bloch, J. Beille, P. Boutron, and J. L. Feron, J. Appl. Phys. **42**, 1679 (1971).

³Vischay, Micro-Measurements, WK 350 AP.

⁴D. S. Rodbell, L. M. Osika, and P. E. Lawrence, J. Appl. Phys. **36**, 666 (1965).

⁵D. Bloch, P. Charbit, and R. Georges, C.R. Acad. Sci. (Paris) **266**, 430 (1968).

⁶B. Morosin, Phys. Rev. B **1**, 236 (1970).

⁷H. Bartholin, D. Bloch, and R. Georges, C.R. Acad. Sci. (Paris) **264**, 360 (1967).

⁸W. L. Roth, Phys. Rev. **110**, 1333 (1958); Phys. Rev. **111**, 772 (1958).

⁹W. L. Roth, Phys. Rev. **31**, 2000 (1960).

¹⁰G. E. Slack, J. Appl. Phys. **31**, 1571 (1960).

¹¹D. Bloch, R. Georges, and I. S. Jacobs, J. Phys. (Paris) **31**, 589 (1970).

¹²R. L. Clendennen and H. G. Drickamer, J. Chem. Phys. **44**, 4223 (1966).

¹³M. F. Cracknell and R. G. Evans, Solid State Commun. **8**, 359 (1970).

¹⁴D. Bloch, J. Phys. Chem. Solids **27**, 881 (1966).

¹⁵V. C. Srivastava, J. Appl. Phys. **40**, 1017 (1969); O. H. Lowndes, Jr., L. Finegold, R. N. Rodgers, and B. Morosin, Phys. Rev. **186**, 515 (1969).

¹⁶M. E. Lines and E. D. Jones, Phys. Rev. **139**, A1313 (1965).

¹⁷J. Kanamori, Prog. Theor. Phys. **17**, 197 (1957).

¹⁸D. S. Rodbell and J. Owen, J. Appl. Phys. **35**, 1002 (1964).

¹⁹M. Bonfante, B. Hennion, F. Moussa, and G. Pepy, Solid State Commun. **10**, 553 (1972).

²⁰L. Néel, C.R. Acad. Sci. (Paris) **203**, 304 (1936).